SCIENTIFIC REPORTS

OPEN

Friction factor for turbulent open channel flow covered by vegetation

Wei-Jie Wang[1,2], Wen-Qi Peng[1,2], Wen-Xin Huai[3], Gabriel G. Katul[4,5], Xiao-Bo Liu[1,2], Xiao-Dong Qu[1,2] & Fei Dong[1,2]
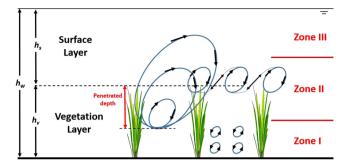
The need for operational models describing the friction factor f in streams remains undisputed given its utility across a plethora of hydrological and hydraulic applications concerned with shallow inertial flows. For small-scale roughness elements uniformly covering the wetted parameter of a wide channel, the Darcy-Weisbach $f = 8(u_*/U_b)^2$ is widely used at very high Reynolds numbers, where u_* is friction velocity related to the surface kinematic stress, $U_b = Q/A$ is bulk velocity, Q is flow rate, and A is cross-sectional area orthogonal to the flow direction. In natural streams, the presence of vegetation introduces additional complications to quantifying f, the subject of the present work. Turbulent flow through vegetation are characterized by a number of coherent vortical structures: (i) von Karman vortex streets in the lower layers of vegetated canopies, (ii) Kelvin-Helmholtz as well as attached eddies near the vegetation top, and (iii) attached eddies well above the vegetated layer. These vortical structures govern the canonical mixing lengths for momentum transfer and their influence on f is to be derived. The main novelty is that the friction factor of vegetated flow can be expressed as $f_v = 4C_d(U_v/U_b)^2$ where U_v is the spatially averaged velocity within the canopy volume, and C_d is a local drag coefficient per unit frontal area derived to include the aforementioned layer-wise effects of vortical structures within and above the canopy along with key vegetation properties. The proposed expression is compared with a number of empirical relations derived for vegetation under emergent and submerged conditions as well as numerous data sets covering a wide range of canopy morphology, densities, and rigidity. It is envisaged that the proposed formulation be imminently employed in eco-hydraulics where the interaction between flow and vegetation is being sought.

Since its inception by Darcy (in 1857) and Weisbach (in 1845), the now called Darcy-Weisbach equation for determining frictional losses in open channels (and pipes) is considered 'standard' provided its associated friction factor coefficient $f = 8(u_*/U_b)^2$ is known, where $u_* = \sqrt{gR_hS_f}$ is the friction velocity related to the kinematic 'bed stress', g is the gravitational acceleration, R_h is the hydraulic radius, S_f is the frictional slope or energy grade-line that converges to the bed-slope S_o for uniform flow, $U_b = Q/A$ is the bulk or time and area-averaged velocity determined from the flow rate Q and cross-sectional area $A = Bh_w$ (assuming rectangular section) orthogonal to the flow direction, B is the channel width and h_w is the water depth approximating R_h when $B \gg h_w$. The definition of f can be combined with the estimate of u_* to yield

$$S_f = \frac{fU_b^2}{8gR_h}.$$

(1)

In classical hydraulics, the work of Moody, Nikuradse and many others established f to vary with two dimensionless quantities: the relative roughness r/R_h and a bulk Reynolds number $Re_{b,h} = U_bR_h/\nu$, where ν is the kinematic viscosity of water. This expression is generally accepted in pipe- and open channel- flows above small-scale roughness elements where $r/h_w \ll 1$. At very high $Re_{b,h}$, f becomes independent of $Re_{b,h}$ and is presumed to abide

[1]State Key Laboratory of Simulation and Regulation of Water Cycle in River Basin, China Institute of Water Resources and Hydropower Research, Beijing, 100038, China. [2]Department of Water Environment, China Institute of Water Resources and Hydropower Research, Beijing, 100038, China. [3]State Key Laboratory of Water Resources and Hydropower Engineering Science, Wuhan University, Wuhan, Hubei, 430072, China. [4]Nicholas School of the Environment, Duke University, Durham, North Carolina, 27708, USA. [5]Department of Civil and Environmental Engineering, Duke University, Durham, North Carolina, 27708, USA. Correspondence and requests for materials should be addressed to W.-Q.P. (email: pwq@iwhr.com)

Figure 1. The key vortical structures in different regions of a vegetated zone in a wide channel where the vegetation is submerged. The vegetation height h_v and the water depth h_w are also presented. The surface (i.e. vegetation free zone) and vegetation layers are defined here.

by the so-called Strickler scaling $f \sim (r/R_h)^{1/3}$[1-3]. An immediate consequence of this result is that when r is a priori known, f and subsequently S_f can be determined from Eq. 1.

Operationally, such an expression for S_f can be used to mathematically close the combined continuity and unsteady shallow water flow equations (i.e., the Saint-Venant) to predict h_w and U_b in a plethora of hydrological and hydraulics applications. Example applications include overland flow from bare to vegetated patches, dam-break and similar shallow inertial flows, flash-flood runoff in ephemeral streams, tsunamis on coastal plains, to name a few[4-11]. It is now recognized that such naive view of f cannot be juxtaposition to streams covered by large roughness values ($r/h_w > 0.1$) such as shallow flow over gravel beds[12-17] or vegetation[18-20] and frames the scope of the work here. In fact, a number of authors are calling for the abandonment of such an approach altogether in such situations[21,22].

The main theoretical novelty is to arrive at a new expression for f whose generic form resembles the conventional $f = 8(u_*/U_b)^2$ for steady-uniform flow through or above dense canopies. Specifically, it is shown that under certain simplifying assumptions, the canopy-related f (hereafter referred to as f_v) is given by

$$f_v = 4C_d \left(\frac{U_v}{U_b} \right)^2 ,$$
(2)

where U_v is the spatially averaged velocity within the canopy volume, and C_d is a local drag coefficient per unit frontal area derived to include the layer-wise effects of vortical structures within and above the canopy along with key vegetation properties. For this expression to be used in practice, an estimate of U_v/U_b and C_d are required. The derivation of Eq. 2 and estimates of C_d and U_v/U_b are first presented followed by a comparison between model predictions and measurements of f_v. Comparisons with other widely used models of f_v are also featured demonstrating that the proposed formulation appears superior to all prior formulations across a wide-range of experiments and canopy-flow configurations.

Background. To progress on the description of f_v for canopy flows, a number of studies have been conducted to explore connections between the shape of the mean velocity profile $u(z)$ and its depth-integrated value defined as

$$U_b \approx \frac{1}{h_w} \int_0^{h_w} u(z)dz,$$
(3)

in wide rectangular channels, where z is the distance from the channel bottom[23-30]. These studies naturally bridge the dominant vortical structures[31,32] to $u(z)$[12,33-35] and subsequently to U_b and f_v. Other studies have focused on the force balance and stresses acting on the vegetation elements as well as R_h to arrive at u_* and f_v[36-38]. Various resistance models for flow within and above vegetated elements were proposed that used bulk flow measurements or combination of models and measurements to determine f[9,39-56]. The emerging picture from all these studies is that key vortical structures impact the shape of $u(z)$ across various canopy layers and in the vegetation free layer for submerged vegetation. The relation between these vortical structures and $u(z)$ is now reviewed.

Review of the mean velocity profile within and above canopies. For stationary and planar-homogeneous flow in a wide channel covered by a densely vegetated canopy, the flow region h_w can be decomposed into three zones according to the dominant sizes of the vortices in each zone as shown in Fig. 1.

Zone I forms near the channel bottom where von Karman vortex streets dominate the energetics of turbulence in the vertical direction. The mean velocity in zone I can be approximated by a constant given as[41,57,58]

$$u_I = \sqrt{\frac{2gS_f}{C_d mD}},$$
(4)

where C_d is a local drag coefficient as before, m is the number of rods or vegetation stems per unit ground area, and D is the frontal width of vegetation elements.

Zone II spans the vegetation top and is dominated by attached eddies to a zero-plane displacement as well as mixing-layer eddies (though those types of eddies do not co-exist in space but both impact time-averaged statistics). When explained by the mixing layer analogy, the mean velocity is given by

$$\frac{u_{II}(z)}{u_{v,top}} = 1 + \tanh\left(\frac{z - h_v}{L_{mix}}\right), \tag{5}$$

where $u_{v,top}$ is the mean velocity at the top of the vegetation elements, h_v is the vegetation height, L_{mix} is a characteristic energetic eddy size generated from Kelvin-Helmholtz instabilities[34].

Zone III resembles a canonical turbulent boundary layer above a rough ground surface and is commonly represented by

$$u_{III}(z) = \frac{u_{*,sur}}{\kappa}\ln\left(\frac{z - d}{z_0}\right), \tag{6}$$

where the friction velocity $u_{*,sur} \approx \sqrt{gh_s S_f}$ for the surface layer (as before) whose thickness is h_s, z_o is the momentum roughness length (linked to r or h_v), d is the zero-plane displacement height and is related to the penetration depth, κ is the von Karman constant, and $h_s = h_w - h_v$ when $h_w/h_v > 1$ (submerged vegetation case).

Due to the presence of vegetation, the addition of zones I and II introduce major distortions to the expected $u(z)$ shape when compared to a typical rough boundary (i.e. zone III) where f_v primarily varies with r/h_w and $Re_{b,h}$ as before. When $r/h_w \ll 1$ (in zone III), r may be linked to z_0 using the scaling relation $r \sim z_o^{1/6}$ discussed elsewhere[12]. The aforementioned distortions to $u(z)$ and the possibility of deriving a general expression for f_v to be used in operational models for emergent and submerged vegetation is the main goal of the work here.

Derivation of a Friction Factor for Vegetated Flow

The goal of the derivation here is to arrive at a new formula for f_v whose generic form resembles the conventional $f = 8(u_*/U_b)^2$ and is given by

$$f_v = 8\left(\frac{u_{*,v}}{U_b}\right)^2 = \frac{8gS_v R_v}{U_b^2}. \tag{7}$$

This definition necessitates estimates of the friction velocity for the vegetated flow $u_{*v} = \sqrt{gS_v R_v}$, where S_v denotes the energy grade-line slope caused by the presence of vegetation, R_v denotes a new vegetation-related hydraulic radius, and U_b is, as before, the bulk flow velocity averaged over the entire cross-sectional area but adjusted for the finite porosity of the vegetation medium.

Section 2.1 derives the vegetation-related energy slope S_v and Section 2.2 derives the vegetation-related hydraulic radius R_v. The outcome is then compared to a wide range of published data sets and prior formulations derived from fitting to other published data sets.

Derivation of vegetation-related energy slope. Throughout, it is assumed that the flow is steady and uniform occurring within a wide rectangular open channel characterized by width B and bed slope S_o. The case considered here is when vegetation is sufficiently dense so that the overall friction factor is mainly due to f_v not bed and side-wall friction and the frictional slope is S_v. The vegetation is further assumed to be cylindrical with height h_v, diameter D, and density m defined by the number of cylinders per unit area as before. The vegetation can be in one of two-states: submerged ($\alpha < 1$) or emergent ($\alpha > 1$) as characterized by the degree of submergence $\alpha = h_v/h_w$. For a control volume above a unit bed area extending from the channel bed to the water surface, the mean momentum balance in the streamwise direction reduces to a force-balance between (i) the gravitational contribution of the water weight along the streamwise direction for a unit ground area ($=F_w$), and (ii) the drag force per unit ground area ($=F_v$) caused by the presence of vegetation stems resisting the flow. The F_w is given by

$$F_w = \rho g S_v V_w, \tag{8}$$

where ρ is the water density, V_w is the volume of flowing water per unit ground area determined from the entire domain volume reduced by the volume occupied by the vegetation elements. The $V_w = h_w(1 - \alpha\phi)$ for submerged conditions (i.e. $\alpha < 1$) and $V_w = h_w(1 - \phi)$ for emergent vegetation (i.e. $\alpha > 1$), where ϕ is the volume fraction of the vegetation. When ignoring wall stresses relative to the drag force imposed by the dense vegetation and assuming a quadratic-law for F_v yields

$$F_v = C_d A_v \frac{\rho U_{ref}^2}{2}, \tag{9}$$

where A_v is frontal area of vegetation given by $A_v = mDh_v$ for $\alpha < 1$ and $A_v = mDh_w$ for $\alpha > 1$, C_d in Eq. (9) is a '*local spatially-averaged*' non-constant drag coefficient that must account for the effects of the vegetation on the flow as discussed elsewhere[55], and U_{ref} is a reference velocity representing the flow within the vegetation section sensing the drag elements. A number of plausible velocities are now introduced to represent U_{ref}: (a) The bulk velocity in the vegetation layer (VL, zones I + II) sensing the drag effects that can be estimated from $U_{v,b} = Q_v/(Bh_v)$[59–61]. (b) The pore velocity in VL calculated based on a spatially-averaged value $U_{v,p} = Q_v/(B_p h_v)$,

where the effective width used for the pore velocity is $B_p = B(1 - \phi)$[36,51,62–65]. (c) The constricted velocity in a classical staggered array $U_{v,c} = Q_v/(B_c h_v)$ with a characteristic constricted width $B_c = B(1 - D/L_{s,stag})$[55], where $L_{s,stag}$ is the spacing distance defined in Etminan *et al.*' work[55]. (d) The separation velocity $U_{v,s} = k_p U_{v,p}$ where k_p is a kinetic energy of a subgrid scale (SGS) for a Smagorinsky model[55]. Due to different vegetation arrangements used in the experiments analyzed here (Section 3 and 4), the spatially-averaged pore velocity was adopted (i.e. $U_{ref} = U_{v,p}$). Detailed analysis shows that this choice of U_{ref} along with a vegetation-related hydraulic radius resulting in a new Reynolds number perform reasonably when compared to many experiments (discussed later). Hence, from the force balance $F_w = F_v$, the vegetation-related friction slope is given by

$$S_v = \frac{C_d A_v}{2g V_w} U_{v,p}^2, \tag{10}$$

where C_d and $U_{v,p}$ remain to be determined.

Derivation of a vegetation-related hydraulic radius R_v. Many studies treat flow resistance of a vegetated canopy as equivalent to a 'bed stress' assuming energy losses occur due to a 'vegetated bed'. This equivalence is convenient as it leads to a hydraulic radius related to flow depth h_w or surface layer depth h_s[9,41,44,66] without considering the details of the vegetation configuration such as frontal area associated with ϕ, m and D. However, the flow resistance by vegetation is mainly dominated by form drag and is directly linked to the frontal area of the rods. The hydraulic radius may be revised to account for these vegetation-related features. Here, a vegetation-related hydraulic radius R_v is proposed by extending the work of Cheng[36] from emergent condition to submerged cases, where the vegetation-related hydraulic radius R_v is now defined by the ratio of the whole flow volume V_w per unit ground area to the vegetation-fluid contact $A_{resistance}$ per unit ground area and can be expressed as

$$R_v = \frac{V_w}{A_{resistance}}. \tag{11}$$

From Eq. (9), the vegetation resistance is caused by its form drag, which is a function of the frontal vegetated area A_v per unit ground area. Hence, the vegetation-related hydraulic radius is

$$R_v = \frac{V_w}{A_v}. \tag{12}$$

Since both V_w and A_v are defined per unit ground area, the ground area cancels in the definition of R_v.

Derivation of the friction formula for flow through submerged and emergent vegetation. The friction factor caused by the presence of vegetation is now obtained by substituting Eqs (10 and 12) into Eq. (7) to yield

$$f_v = 4C_d \left(\frac{U_v}{U_b}\right)^2. \tag{13}$$

This expression is similar to a prior result given by[9]

$$f_{v,poggi} = 4\left(\frac{L_c}{h_v}\right)^{-1} \left[1 + \left(1 - \frac{1}{\alpha}\right)\frac{\Delta U}{U_v}\right]^{-2}, \tag{14}$$

derived from a different set of assumptions. To illustrate the similarities between the two expressions, consider the canopy-level adjustment length scale $L_c = (C_d m D)^{-1}$ as defined by the aforementioned study and $\Delta U = U_s - U_v$ to be the velocity difference between the vegetation zone U_v and the free water zone U_s. Equation (14) can be arranged to read $f_{v,poggi} = 4C_d m D h_v (U_v/U_b)^2$, where C_d is a local drag coefficient per unit frontal area (as shown next). More relevant here is that Eq. (13) allows for multiple effects to be conveniently included in a dimensionless C_d (instead of a dimensional L_c) and U_v/U_b. Before doing so, it is to be noted that when submergence $\alpha = h_v/h_w \ll 1$[44], $U_v \sim u_*$ and the conventional expression for friction factor is recovered from Eq. (13). To show explicitly similarities and differences between Eqs (13 and 14), the force balance for submerged conditions is rewritten per unit ground area as

$$\rho g S_f R_h = \tau_{v,poggi}, \tag{15}$$

so that

$$\rho g S_f \left[h_w(1 - \alpha\phi)\right] = C_d (m D h_v)\frac{\rho U_v^2}{2}, \tag{16}$$

where C_d is a local drag coefficient per unit frontal area as before. Equation (14) further assumes the hydraulic radius to be the flow depth, or $R_h = h_w(1 - \alpha\phi) \approx h_w$. Using this definition of $\tau_{v,poggi} = C_d m D h_v \rho U_v^2/2$ and inserting this definition into the definition of $f = 8\tau/(\rho U_b^2)$ yields $f_{v,poggi} = 4C_d m D h_v (U_v/U_b)^2$. However, when

using a vegetation-related hydraulic radius $R_v = V_w/A_v = h_w(1 - \alpha\phi)/(mDh_v)$ instead of R_h as proposed here, Eq. (16) can be transformed as

$$\rho g S_f \left[\frac{h_w(1 - \alpha\phi)}{mDh_v} \right] = C_d \frac{\rho U_v^2}{2},$$

(17)

and the expression

$$\rho g S_f R_v = \tau_{v,present},$$

(18)

is recovered where C_d remains a local drag coefficient per unit frontal area (as before). Naturally, when setting $\tau_{v,present} = C_d \rho U_v^2/2$ into the definition of $f = 8\tau/(\rho U_b^2)$, the outcome $f_{v,present} = 4C_d(U_v/U_b)^2$ of Eq. (13) is recovered. It can be surmised that different R_h definitions yield expressions for f that appear to be different. However, not withstanding these apparent differences, the C_d remains a local drag coefficient per unit frontal area in all of them.

Because C_d is to be related to a local Reynolds number, several possibilities are now reviewed for defining a local Reynolds number in the presence of vegetation. Etminan *et al.*[55] compared Reynolds numbers using various characteristic velocity scales ($U_{v,b}$, $U_{v,p}$, $U_{v,c}$ and $U_{v,s}$) with a fixed characteristic length scale D giving $Re_{v,b}$, $Re_{v,p}$, $Re_{v,c}$ and $Re_{v,s}$. The aforementioned work then showed that typical C_d formulation for a single cylinder can be employed to predict a drag coefficient for staggered vegetation when using $U_{v,c}$ as the reference velocity to form $Re_{v,c} = U_{v,c}D/\nu$ and resulting in a best-fit expression applicable for $0 < Re_{v,c} < 6000$ given as

$$C_{d,ELG} = 1 + 10Re_{v,c}^{-2/3},$$

(19)

where suffix 'ELG' denotes the first letter of the surname of each author in Etminan *et al.*[55]. Here, vegetation effects are introduced in both velocity and length scales by selecting the pore velocity (U_v or U_b) and the vegetation-related hydraulic radius R_v for defining a Reynolds number. For emergent canopies, only the canopy layer exists and the Reynolds number is labeled as $Re_{v,v}$ (in the suffix, the first letter 'v' is vegetation layer, and second letter 'v' denotes the characteristic length in the Reynolds number to be the vegetation-related hydraulic radius) given as

$$Re_{v,v} = \frac{U_v R_v}{\nu},$$

(20)

where R_v is the vegetation-related hydraulic radius as before, given as

$$R_v = \frac{\pi D(1 - \phi)}{4\phi}.$$

(21)

For a submerged vegetation, the Reynolds number $Re_{b,v}$ can also be defined as (in the suffix the first letter 'b' is bulk flow, and second letter 'v' denotes the characteristic length in the Reynolds number to be vegetation-related hydraulic radius)

$$Re_{b,v} = \frac{U_b R_v}{\nu},$$

(22)

where R_v is, as before, the vegetation-related hydraulic radius now given as

$$R_v = \frac{\pi D(1 - \alpha\phi)}{4\alpha\phi}.$$

(23)

Friction Factor for Flow Through Emergent Vegetation

For emergent vegetation in flow ($h_v > h_w$)

$$f_v = 4C_d,$$

(24)

Cheng's result[36] for emergent vegetated flow is recovered. In the aforementioned study, f was shown to be a monotonically decreasing function of Reynolds number $Re_{v,v}$ consistent with several studies[29,39,59,62,63,67,68]. The relation between f and Reynolds number is analyzed using several experiments described next.

Laboratory experiments. *Present study.* Flume experiments were conducted in a 10 m long and $B = 0.3$ m wide glass flume at the State Key Laboratory of Water Resources and Hydro-power Engineering Science at Wuhan University in China. The flume bed was set flat and the vegetation stems were arranged in linear configuration to ensure a locally uniform resistance. The vegetation was composed of cylinders with diameter $D = 8$ mm and height $h_v = 250$ mm. The cylindrical vegetation array was then positioned on a 10 mm thick plastic board covered with holes to allow for variable cylinder density variation (or m). Let $\phi_{board} = m_0 \pi D^2/4$ be the fractional area covered by holes on the bare board with m_0 being the number of holes on the bare board per unit board area being used for each run. Eight vegetation densities were then used, labeled Runs A to H, with $\phi = 0.419$, 0.291, 0.206, 0.163, 0.073, 0.041, 0.018 and 0.010, respectively. For all the runs, steady non-uniform flow was conducted with constant flow rate $Q = 0.00384$ m$^3 s^{-1}$.

Authors	ϕ (%)	D (m)	U_v (m/s)	$Re_{v,v}$	C_d
Present study	1.0–41.9	0.008	0.144–0.306	1256–190530	1.04–1.54
Ishikawa et al.[59]	0.3–3.2	0.004–0.0064	0.165–0.908	24883–904213	0.56–1.29
Tanino and Nepf[62]	9.0–35.0	0.0064	0.004–0.105	54–5266	1.54–9.65

Table 1. Summary for emergent vegetation in flow.

A local $C_{d,local} - Re$ function in steady non-uniform flow was derived and shown to be parabolic in shape (i.e. not monotonic) within the vegetation zone for a given vegetation density. Here, the focus is on the averaged drag for the entire vegetation zone, which can be expressed as

$$C_d = \int_0^1 C_{d,local}(x^+)\, dx^+ \tag{25}$$

where $C_{d,local}$ is a local drag coefficient that varies in the streamwise direction along the vegetation zone, the normalized distance is $x^+ = x/L_{veg}$ along the streamwise direction, and L_{veg} is the streamwise length of the vegetation zone. A summary of the data used here is given in Table 1 and the details are shown in Supplementary Information (Table S1). Also, further details about the experimental setup can be found elsewhere[51].

Two other published data sets from Ishikawa et al.[59] and Tanino et al.[62] are used here and are briefly summarized in Table 1.

Experiments conducted by Ishikawa et al. The first data set was generated from a 15 m long, 0.3 m wide, and 0.3 m deep channel using two types of steel cylinders with diameters 0.004 m and 0.0064 m, and a height of 0.2 m as described elsewhere[59]. The cylinder spacing was uniform in each case (=0.0632 m and 0.0316 m, respectively). The flow was nearly uniform and the steel canopy array was arranged in staggered configuration. The hydraulic parameters required here are given in Supplementary Information (Table S1).

Experiments conducted by Tanino et al. Tanino et al.[62] conducted their experiments in two Plexiglas recirculating flumes. Cylindrical maple dowels with diameter $D = 0.0064$ m were used as laboratory models for vegetation. The vegetation array fractional volume varied as $\phi = 0.091, 015, 0.20, 0.27, 0.35$. The following data points (shown in Supplementary Information Table S1) were tracked from their best-fitting curve to yield an approximate expression

$$C_{d,tn} = 2\left(\frac{T_1}{Re_d} + T_2\right), \tag{26}$$

where suffix 'tn' denotes the expression of Tanino et al.[62], T_1 and T_2 are obtained from linear regression. The $Re_{v,d}$ in their formulation was based on a stem Reynolds number given as

$$Re_{v,d} = \frac{U_v D}{\nu}, \tag{27}$$

which uses D as characteristic length for their Reynolds number.

Empirical expressions. For flow through emergent vegetation, a large synthesis study proposed a $C_d - Re$ expression given as[36]

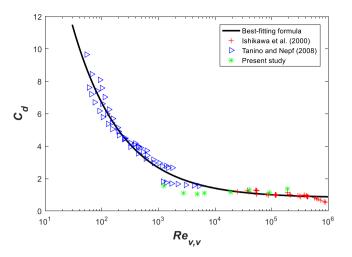$$C_{d,cheng} = \frac{50}{Re_{v,v}} + 0.7\left[1 - \exp\left(-\frac{Re_{v,v}}{15000}\right)\right]. \tag{28}$$

The linkage between vegetation-array and stem related Reynolds number is

$$Re_{v,v} = \frac{R_v}{D} Re_{v,d} = \frac{\pi(1-\phi)}{4\phi} Re_{v,d}. \tag{29}$$

Here, a simplified expression that summarizes all the aforementioned expressions may be expressed as a function of $Re_{v,v}$ (desirable for the purposes of the work here) as

$$C_d = 0.819 + \frac{58.5}{\sqrt{Re_{v,v}}}. \tag{30}$$

This summary expression is shown in Fig. 2, which an be re-arranged to be related to the more commonly reported $Re_{v,d}$ as

Figure 2. Best-fit expression for the local $C_d - Re_{v,v}$ relation for the emergent vegetation case.

$$C_d = 0.819 + \frac{58.5}{\sqrt{\frac{\pi(1-\phi)}{4\phi}Re_{v,d}}}.$$

(31)

Based on this drag coefficient, the f for emergent vegetation is given as a function of $Re_{v,v}$

$$f_{v,emergent} = 3.276 + \frac{234}{\sqrt{Re_{v,v}}},$$

(32)

or as a function of $Re_{v,d}$

$$f_{v,emergent} = 3.276 + \frac{234}{\sqrt{\frac{\pi(1-\phi)}{4\phi}Re_{v,d}}}.$$

(33)

Friction Factor for Flow Through Submerged Vegetation

Laboratory experiments. For submerged vegetated flow, data were used from several published experiments and classified as either rigid or flexible. Data for the rigid vegetation flow are described elsewhere[29,31,38,57,69–76]. Data for flexible vegetation are also described elsewhere[24,69,76–81]. A summary of all the data points are in Table 2 and the details can be found in Supplementary Information (Tables S2 and S3).

Determination of depth-averaged velocity in the vegetation and surface layers. In the vegetation layer (VL), the depth-averaged velocity can be derived based on the force balance between vegetation drag and flow gravity in streamwise direction

$$U_v = \sqrt{\frac{2gS_o(1-\alpha\phi)}{C_d mD\alpha}},$$

(34)

where C_d is calculated from Eqs (30 or 31), indicating iterations are needed to obtain the velocity and drag coefficient. Moreover, the effective width of the canopy layer for the pore velocity $B_p < B$ is briefly discussed. Figure 3 shows side and top views of the flume with cylindrical vegetation, where the green zone indicates the area occupied by vegetation. The effective width B_p is expressed as $B_p = B(1-\phi)$.

For surface layer (SL), the depth-averaged velocity can be determined by the linkage between the vegetation-layer velocity U_v and the bulk velocity U_b. The bulk velocity is defined by the total discharge Q to the effective cross-sectional area and given as (pore velocity for bulk flow)

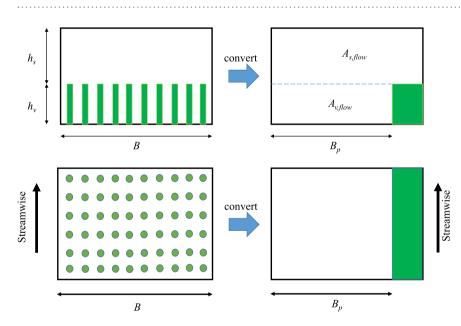$$U_b = \frac{Q}{A_e} = \frac{Q}{h_s B + h_v B(1-\phi)}.$$

(35)

From the continuity equation,

$$Q = Q_s + Q_v = U_s A_{s,flow} + U_v A_{v,flow},$$

(36)

where Q_s, $A_{s,flow}$ are the flow rate and the effective cross-sectional area in the surface layer, and Q_v, $A_{v,flow}$ are the flow rate and the effective cross-sectional area in the vegetation layer. The relation between U_b, U_s and U_v is derived as

Vegetation type	Authors	Q (m³ s⁻¹)	B (m)	H (m)	S_o (%)	ϕ (%)	D (m)	h_v (m)	m (stems m⁻²)
Rigid vegetation	Dunn[69]	0.046–0.181	0.91	0.164–0.391	0.36–1.61	0.14–1.23	0.006	0.118	43–387
	Ghisalberti and Nepf[31]	0.002–0.014	0.38	0.467	0.0002–0.01	1.26–4.02	0.006	0.138–0.139	391–1250
	Liu et al.[29]	0.011	0.30	0.087–0.119	0.30	0.31–1.57	0.006	0.076	97–496
	López and García[70]	0.046–0.181	0.91	0.164–0.391	0.36–1.61	0.14–1.24	0.006	0.12	42–384
	Meijer[71]	0.866–8.98	3.00	0.990–2.500	0.055–0.205	0.32–1.29	0.008	0.45–1.5	64–256
	Murphy et al.[72]	0.002–0.014	0.38	0.088–0.467	0.0003–0.1340	1.18–3.77	0.006	0.070–0.140	417–1333
	Nezu and Sanjou[38]	0.003–0.008	0.40	0.063–0.200	0.0196–0.1553	4.76–18.48	0.008	0.050	947–3676
	Poggi et al.[57]	0.162	0.90	0.600	0.004–0.0320	0.08–1.35	0.004	0.12	67–1072
	Shimizu et al.[73]	0.002–0.016	0.40–0.50	0.050–0.106	0.0660–0.7000	0.44–0.79	0.01–0.02	0.041–0.046	2501–9995
	Stone and Shen[74]	0.002–0.065	0.45	0.151–0.314	0.009–4.400	0.55–6.11	0.003–0.013	0.124	166–692
	Yan[75]	0.014–0.038	0.42	0.120–0.300	0.065–1.280	1.41–5.65	0.006	0.06	500–2000
	Yang and Choi[76]	0.008–0.011	0.45	0.075	0.141–0.269	0.44	0.002	0.035	1400
Flexible vegetation	Dunn[69]	0.078–0.180	0.91	0.230–0.367	0.36–1.01	0.14–1.23	0.006	0.097–0.161	43–388
	Yang and Choi[76]	0.008–0.011	0.45	0.055–0.110	0.07–0.361	0.44	0.002	0.023–0.034	1400
	Kubrak et al.[77]	0.027–0.075	0.58	0.180–0.266	0.87–1.74	0.13–0.53	0.001	0.131–0.164	2500–10000
	Okamoto and Nezu[78]	0.006–0.032	0.40	0.150–0.315	0.019–0.2409	4.78	0.008	0.03–0.096	951
	Järvelä[79]	0.040–0.143	1.10	0.306–0.707	0.02–0.36	7.39	0.003	0.155–0.260	12000
	Carollo et al.[80]	0.027–0.189	0.60	0.119–0.277	0.2–1.0	2.2–3.46	0.001	0.031–0.082	28000–44000
	Ciraolo and Ferreri[24]	0.027–0.177	0.77	0.150–0.478	0.008–0.85	2.04	0.005	0.063–0.290	1037
	Kouwen et al.[81]	0.003–0.142	0.61	0.149–0.400	0.05–1.0	9.82	0.005	0.050–0.100	5000

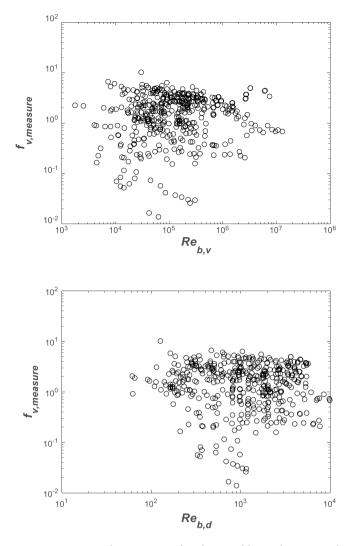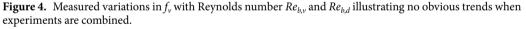**Table 2.** Summary for submerged vegetation flow.

Figure 3. Side and top views of submerged vegetation flow and the definition of effective width B_p from the geometric width B.

$$U_b = \frac{U_s h_s + U_v h_v (1 - \phi)}{h_s + h_v (1 - \phi)}. \tag{37}$$

Arranging the above equation, the bulk velocity is given by

$$U_b = \frac{1 - \alpha}{1 - \alpha\phi} U_s + \frac{\alpha(1 - \phi)}{1 - \alpha\phi} U_v, \tag{38}$$

Figure 4. Measured variations in f_v with Reynolds number $Re_{b,v}$ and $Re_{b,d}$ illustrating no obvious trends when experiments are combined.

then the depth-averaged velocity of surface layer gives

$$U_s = \frac{(1 - \alpha\phi)}{1 - \alpha} U_b - \frac{\alpha(1 - \phi)}{1 - \alpha} U_v. \tag{39}$$

Methods to determine friction factor in the submerged cases. The measured friction $f_{v,measure}$ can be obtained from U_v (using Eq. 34), U_b (using Eq. 35) and C_d (using Eqs 30 or 31) when setting $f_v = 4C_d(U_v/U_b)^2$. All data points and their variation with the Reynolds number $Re_{b,v}$ or $Re_{b,d}$ are given in Fig. 4. The results suggest no obvious trends between measured f_v and estimated $Re_{b,v}$ or $Re_{b,d}$.
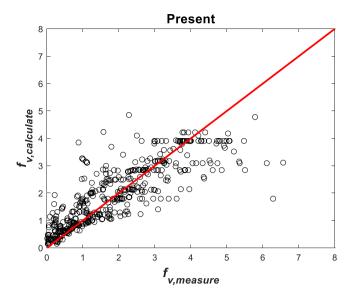
The absence of a unique relation between f_v and Reynolds number requires further inquiry. The key to calculating f_v is U_v/U_b. Previous studies[9] showed that f_v is linked to two dimensionless groups: $\alpha = h_v/h_w$ and $\eta = h_v/L_c$. As mentioned before, the adjustment canopy length scale is defined as

$$L_c = \frac{1}{C_d m D}. \tag{40}$$

The aforementioned study[9] did show a nonlinear increase in f_v with increasing α at a given η, and a nonlinear increase in f_v with increasing η at a given α. Based on these results, we propose a 3-parameter mathematical function to describe this behavior without focusing on the detailed mean velocity profile in each zone. This 3-parameter function is given as

$$\left(\frac{U_v}{U_b}\right)^2 = \frac{p_1\alpha^2}{p_2\alpha + p_3\eta} \tag{41}$$

Figure 5. Comparison between measured and predicted f_v for all the data sets combined.

where p_1, p_2, p_3 are constants to be determined from regression analysis. The corresponding friction f_v can now be expressed as

$$f_{v,present} = 4C_d\left(\frac{p_1\alpha^2}{p_2\alpha + p_3\eta}\right).$$

(42)

This equation shows f_v increases with increasing submergence $\alpha = h_v/h_w$ when other parameters are held constant, and increases with increasing $\eta = h_v/L_c$ when other parameters are held constant. With a local C_d determined from Eq. (31), parameters $p_1 = 1.198$, $p_2 = 0.681$, $p_3 = 0.416$ where determined using non-linear regression with a correlation coefficient $R_{cc} = 0.803$ as shown in Fig. 5.

Friction factor derived from previous studies. Some studies report expressions for the velocity within the vegetated zone, which can also be used to obtain a friction factor. A summary of these expressions are briefly reviewed. Stone *et al.*[74] estimated the bulk velocity as

$$U_b = 1.385\left(\frac{1}{\alpha}\sqrt{\frac{\pi}{4\phi}} - 1\right)\sqrt{gDS_f}.$$

(43)

Baptist *et al.*[41] report a bulk velocity as

$$U_b = \left[\sqrt{\frac{1}{g/C_b^2 + 2C_d\phi h_v/(\pi D)}} + \frac{5}{2}\ln\left(\frac{1}{\alpha}\right)\right]\sqrt{gh_w S_f},$$

(44)

where C_d is the bed-related Chezy coefficient ($=60\,\mathrm{m}^{1/2}\,\mathrm{s}^{-1}$ for smooth bed).

Huthoff *et al.*[28] proposed a

$$U_b = \left[(1-\alpha)\left(\frac{h_s}{D\sqrt{\pi/(4\phi)} - D}\right)^{\frac{2}{3}[1-\alpha^5]} + \sqrt{\alpha}\right]\sqrt{\frac{\pi gDS_f}{2C_d\phi}}.$$

(45)

Yang *et al.*[82] showed a bulk velocity given as

$$U_b = \sqrt{\frac{\pi gDS_f}{2C_d\alpha\phi}} + \frac{C_u\sqrt{gh_s S_f}}{\kappa}\left(\ln\frac{1}{\alpha} + \alpha - 1\right),$$

(46)

where $C_u = 1$ for $4\phi/(\pi D) \leq 5$ and $C_u = 2$ for $4\phi/(\pi D) > 5$.

Cheng *et al.*[83] derived the representative roughness height of the vegetation for the surface layer and proposed

$$U_b = \left[\sqrt{\frac{\pi D(1-\phi)^3}{2C_d\phi h_v}}\alpha^{3/2} + 4.54\left(\frac{h_s}{D}\frac{1-\phi}{\phi}\right)^{1/16}(1-\alpha)^{3/2}\right]\sqrt{gh_w S_f}.$$

(47)

Katul *et al.*[44] proposed an analytical model for U_b linked to three canonical length scales (L_c, h_v, h_w) and is given as

$$U_b = \alpha U_{KCL} + (1 - \alpha) U_{KSL}, \tag{48}$$

where U_{KCL}, U_{KSL} are layer-averaged velocity for the canopy and surface layers, respectively, given as

$$U_{KCL} = \frac{2\beta}{\eta}\left[1 - \exp\left(-\frac{\eta}{2\beta^2}\right)\right]\sqrt{gh_sS_f}, \tag{49}$$

and

$$U_{KSL} = \frac{1}{\kappa}\left\{-1 + \ln\left[\left(\frac{h_w - D}{z_0}\right)^{(h_w-D)/h_s}\left(\frac{h_v - D}{z_0}\right)^{-(h_v-D)/h_s}\right]\right\}\sqrt{gh_sS_f}, \tag{50}$$

where $\beta = min(0.135\sqrt{mD}, 0.33)$ is a momentum absorption coefficient, and z_0 is given by

$$z_0 = \frac{2\beta L_c}{\kappa}\exp\left(-\frac{\kappa}{\beta}\right). \tag{51}$$

With these mean velocity profile formulations, friction factor can be estimated. The bulk velocity of the vegetation layer is determined using Eq. (34) and the velocity across h_w is calculated based on Eqs (43 to 48).

Comparison between measured and modeled friction factor using published bulk velocities.
The different methods are now used to predict f_v and are then compared with measured f_v in Fig. 6. To assess the agreement between prediction and measurement, R_{cc} is computed and reported in Table 3. Figure 6 suggests that the present model performs 'no worse' than other (more elaborate) methods. In many cases, it even outperforms prior methods.

Discussion and Conclusion
Equation $f_v = 4C_d(U_v/U_b)^2$ encodes much of the recent developments about vegetation effects on local drag (e.g. blockage and sheltering, weak Reynolds number dependence, etc) and their up-scaled contribution on f_v via U_v/U_b. These effects are now briefly discussed. For isolated cylinders, the local C_d can be determined from Cheng[43]

$$C_{d,iso} = 11Re_{v,d}^{-0.75} + 0.9\Gamma_1(Re_{v,d}) + 1.2\Gamma_2(Re_{v,d}), \tag{52}$$

where

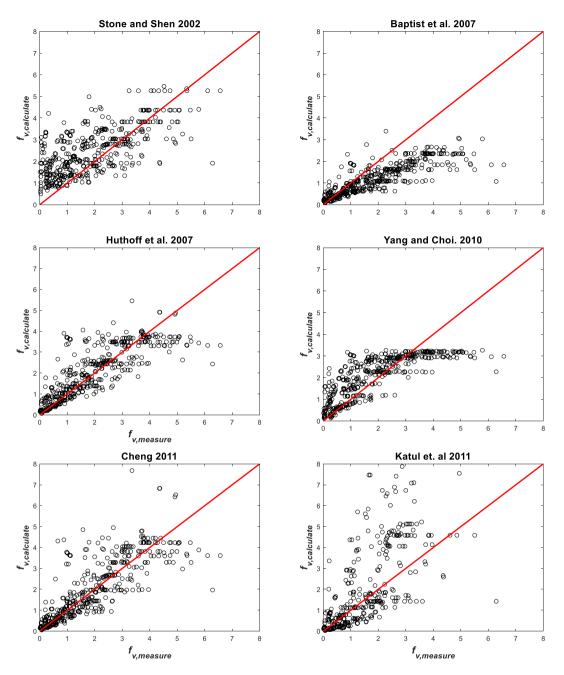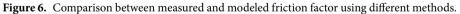$$\Gamma_1(Re_{v,d}) = 1 - \exp\left(-\frac{1000}{Re_{v,d}}\right), \tag{53}$$

and

$$\Gamma_2(Re_{v,d}) = 1 - \exp\left[-\left(\frac{Re_{v,d}}{4500}\right)^{0.7}\right]. \tag{54}$$

Many studies found that C_d in a vegetated array differs from $C_{d,iso}$. When only focusing on variations in vegetation density, C_d appears to increase[62,68] and then decrease[60,84] with increasing vegetation density[55]. In the present study, we go beyond vegetation density and introduce all the key vegetation effects in a Reynolds number $Re_{v,v} = U_vR_v/\nu$ formed by U_v and R_v. These velocity and length scales contain the vegetation density ϕ and appear to collapse the experiments onto a single curve.

To accommodate the mechanics of sheltering, delayed separation and blockage effects arising from an array of cylinders instead of isolated cylinders, C_d of Eq. (31) can be used. Sheltering effect indicates that some elements were located in the wake region of the upstream elements[85], resulting in a lower velocity than their upstream counterparts and generate a lower drag compared with the isolated cylinder case. Delayed separation can be explained by the enhancement of the mean separation angle that is larger than that for the isolated cylinder, resulting in a decreasing drag coefficient (compared with the isolated cylinder). Both sheltering and delayed separation tend to reduce drag when compared to the isolated cylinder case. For the blockage effect, which leads to a local increase in the drag coefficient, it can by explained by two main factors[55], one is that the velocity between cylinders is enhanced by the presence of the vegetation in flow. The other factor is reduced wake pressure[86].

The $C_{d,iso}$ is a local drag coefficient acting on a single stem per unit frontal area without considering the interaction among elements in a vegetation array. To illustrate the role of sheltering, delayed separation and blockage on C_d, a 'bifurcation' type Reynolds number $Re_{v,d}^+$ may be introduced. When $Re_{v,d} < Re_{v,d}^+$, the viscous boundary layer formed around cylinders creates a slow-moving flow zone with a path smaller than the spacing between adjacent stem. This effect leads to an equivalent local drag coefficient by the array of cylinders to be larger than the one associated with isolated cylinders (i.e. a blockage effect). However, when $Re_{v,d} > Re_{v,d}^+$, vegetation stems become a new source of turbulent kinetic energy (wake production) spawning horizontal vortices resembling von
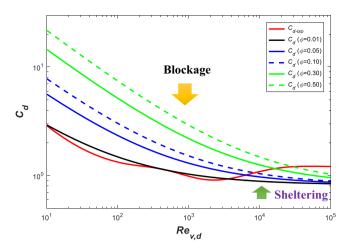
Figure 6. Comparison between measured and modeled friction factor using different methods.

Authors	Correlation coefficient R_{cc}
Present study	0.803
Stone and Shen[74]	0.654
Baptist et al.[41]	0.806
Huthoff et al.[28]	0.790
Yang and Choi[82]	0.758
Cheng[83]	0.783
Katul et al.[44]	0.637

Table 3. Comparison between measured and modeled friction factor by different formulations.

Figure 7. Comparison between local $C_{d,iso}$ and C_d for different vegetation concentration.

Karman streets that grow in size and 'fill' the space between the stems. This effect is akin to a decreasing drag coefficient when compared with $C_{d,iso}$ (i.e. sheltering effect). Blockage and sheltering effects can be distinguished by calculating

$$E = \frac{C_d}{C_{d,iso}}. \tag{55}$$

When $E > 1$, blockage dominates and when $E < 1$, sheltering dominates C_d[51]. Using Eqs ([31] and [52]) with different vegetation concentration ($\phi = 0.01$, 0.05, 0.1, 0.3 and 0.5), blockage and sheltering can be delineated for $Re_{v,d}$ ranging from 10^1 to 10^5 in Fig. [7]. As expected, C_d increases with increasing ϕ for small ϕ. The threshold Reynolds number $Re_{v,d}^+$ also increases with increasing ϕ. For example, at $Re_{v,d}^+ \approx 4000$, separation between blockage and sheltering occurs for $\phi = 0.01$. This threshold $Re_{v,d}^+$ becomes much larger, around 30000 for $\phi = 0.5$. For $\phi = 0.01$, when $Re_{v,d} < Re_{v,d}^+$, the C_d for isolated stems are comparable but not identical to their array counterpart.

To conclude, the expression of friction factor proposed here does accommodate blockage or sheltering through a local drag coefficient C_d (Eq. [31]) and any distortions to the shape of the mean velocity profile (Eq. [41]). Evaluated using numerous data sets covering a wide range of canopy morphology, densities and rigidity, the friction factor for emergent vegetation is shown to be proportional to the drag coefficient. This finding shows why the friction factor monotonically decreases with increasing Reynolds number for emergent vegetation. For submerged vegetation, the friction factor is shown to vary with submergence and adjustment length scale. Also, this variation is not monotonic with increasing Reynolds number.

References

1. Strickler, A. Beitrge zur frage der geschwindigkeitsformel und der rauhigkeitszahlen fr strme, kanle und geschlossene leitungen. *Mitteilungen des Amtes fr Wasserwirtschaft* (1923).
2. Gioia, G. & Bombardelli, F. Scaling and similarity in rough channel flows. *Physical review letters* **88**, 014501 (2002).
3. Bonetti, S., Manoli, G., Manes, C., Porporato, A. & Katul, G. G. Mannings formula and stricklers scaling explained by a co-spectral budget model. *Journal of Fluid Mechanics* **812**, 1189–1212 (2017).
4. Ajayi, A. E., van de Giesen, N. & Vlek, P. A numerical model for simulating hortonian overland flow on tropical hillslopes with vegetation elements. *Hydrological Processes* **22**, 1107–1118, https://doi.org/10.1002/hyp.6665 (2008).
5. Chanson, H., Jarny, S. & Coussot, P. Dam break wave of thixotropic fluid. *Journal of Hydraulic Engineering* **132**, 280–293 (2006).
6. Chanson, H. Application of the method of characteristics to the dam break wave problem. *Journal of Hydraulic Research* **47**, 41–49 (2009).
7. Daly, E. & Porporato, A. Similarity solutions of nonlinear diffusion problems related to mathematical hydraulics and the fokker-planck equation. *Physical Review E* **70**, 056303 (2004).
8. Hogg, A. J. & Pritchard, D. The effects of hydraulic resistance on dam-break and other shallow inertial flows. *Journal of Fluid Mechanics* **501**, 179–212 (2004).
9. Poggi, D., Krug, C. & Katul, G. G. Hydraulic resistance of submerged rigid vegetation derived from first-order closure models. *Water Resources Research* **45**, https://doi.org/10.1029/2008WR007373 (2009).
10. Thompson, S., Katul, G., Konings, A. & Ridolfi, L. Unsteady overland flow on flat surfaces induced by spatial permeability contrasts. *Advances in Water Resources* **34**, 1049–1058, https://doi.org/10.1016/j.advwatres.2011.05.012 (2011).
11. Paschalis, A., Katul, G. G., Fatichi, S., Manoli, G. & Molnar, P. Matching ecohydrological processes and scales of banded vegetation patterns in semi-arid catchments. *Water Resources Research* 1–68, https://doi.org/10.1002/2015WR017679 (2016).
12. Katul, G. G., Wiberg, P., Albertson, J. & Hornberger, G. A mixing layer theory for flow resistance in shallow streams. *Water Resources Research* **38**, https://doi.org/10.1029/2001WR000817 (2002).
13. Manes, C., Pokrajac, D. & McEwan, I. Double-averaged open-channel flows with small relative submergence. *Journal of Hydraulic Engineering* **133**, 896–904 (2007).
14. Manes, C., Poggi, D. & Ridolfi, L. Turbulent boundary layers over permeable walls: scaling and near-wall structure. *Journal of Fluid Mechanics* **687**, 141–170 (2011).
15. Manes, C., Ridolfi, L. & Katul, G. A phenomenological model to describe turbulent friction in permeable-wall flows. *Geophysical research letters* **39** (2012).

16. Lamb, M. P., Brun, F. & Fuller, B. M. Hydrodynamics of steep streams with planar coarse-grained beds: Turbulence, flow resistance, and implications for sediment transport. *Water Resources Research* **53**, 2240–2263 (2017).

17. Ali, S. Z. & Dey, S. Impact of phenomenological theory of turbulence on pragmatic approach to fluvial hydraulics. *Physics of Fluids* **30**, 045105 (2018).

18. Nepf, H. M. Flow and transport in regions with aquatic vegetation. *Annual Review of Fluid Mechanics* **44**, 123–142, https://doi.org/10.1146/annurev-uid-120710-101048 (2012).

19. Wang, W.-J. *et al*. Roughness height of submerged vegetation in flow based on spatial structure. *Journal of Hydrodynamics* **30**, 754–757, https://doi.org/10.1007/s42241-018-0060-3 (2018).

20. Wang, W.-J. *et al*. Derivation of canopy resistance in turbulent flow from first-order closure models. *Water* **10**, 1782, https://doi.org/10.3390/w10121782 (2018).

21. Bjerklie, D. M., Dingman, S. L. & Bolster, C. H. Comparison of constitutive flow resistance equations based on the manning and chezy equations applied to natural rivers. *Water resources research* **41** (2005).

22. Ferguson, R. Time to abandon the manning equation? *Earth Surface Processes and Landforms* **35**, 1873–1876 (2010).

23. Cheng, N.-S. Single-layer model for average flow velocity with submerged rigid cylinders. *Journal of Hydraulic Engineering* **141**, 06015012, https://doi.org/10.1061/(ASCE)HY.1943-7900.0001037 (2015).

24. Ciraolo, G. & Ferreri, G. Log velocity profile and bottom displacement for a flow over a very flexible submerged canopy. In *Proceedings of 32nd Congress of IAHR Harmonizing the Demands of Art and Nature in Hydraulics*, 1–13 (International Association for Hydro-Environment Engineering and Research, Venice, Italy, 2007).

25. Dijkstra, J. & Uittenbogaard, R. Modeling the interaction between flow and highly flexible aquatic vegetation. *Water Resources Research* **46**, https://doi.org/10.1029/2010WR009246 (2010).

26. Wang, W.-J., Huai, W.-X., Zeng, Y.-H. & Zhou, J.-F. Analytical solution of velocity distribution for flow through submerged large deflection flexible vegetation. *Applied Mathematics and Mechanics* **36**, 107–120, https://doi.org/10.1007/s10483-015-1897-9 (2015).

27. Huai, W.-X., Wang, W.-J. & Zeng, Y.-H. Two-layer model for open channel flow with submerged flexible vegetation. *Journal of Hydraulic Research* **51**, 708–718, https://doi.org/10.1080/00221686.2013.818585 (2013).

28. Huthoff, F., Augustijn, D. & Hulscher, S. J. Analytical solution of the depth-averaged flow velocity in case of submerged rigid cylindrical vegetation. *Water Resources Research* **43**, https://doi.org/10.1029/2006WR005625 (2007).

29. Liu, D., Diplas, P., Fairbanks, J. D. & Hodges, C. C. An experimental study of flow through rigid vegetation. *Journal of Geophysical Research*: *Earth Surface* **113**, https://doi.org/10.1029/2008JF001042 (2008).

30. Liu, Z. W., Chen, Y. C., Zhu, D. J., Hui, E. Q. & Jiang, C. B. Analytical model for vertical velocity profiles in flows with submerged shrub-like vegetation. *Environmental Fluid Mechanics* **12**, 341–346, https://doi.org/10.1007/s10652-012-9243-6 (2012).

31. Ghisalberti, M. & Nepf, H. M. The limited growth of vegetated shear layers. *Water Resources Research* **40**, https://doi.org/10.1029/2003WR002776 (2004).

32. Brunet, Y. & Irvine, M. The control of coherent eddies in vegetation canopies: streamwise structure spacing, canopy shear scale and atmospheric stability. *Boundary-Layer Meteorology* **94**, 139–163, https://doi.org/10.1023/A:1002406616227 (2000).

33. Rowinski, P. & Kubrak, J. A mixing-length model for predicting vertical velocity distribution in flows through emergent vegetation. *Hydrological sciences journal* **47**, 893–904, https://doi.org/10.1080/02626660209492998 (2002).

34. Raupach, M., Finnigan, J. & Brunei, Y. Coherent eddies and turbulence in vegetation canopies: the mixing-layer analogy. *Boundary-Layer Meteorology* **78**, 351–382, https://doi.org/10.1007/BF00120941 (1996).

35. Ghisalberti, M. & Nepf, H. M. Mixing layers and coherent structures in vegetated aquatic flows. *Journal of Geophysical Research* **107**, 3011, https://doi.org/10.1029/2001JC000871 (2002).

36. Cheng, N.-S. & Nguyen, H. T. Hydraulic radius for evaluating resistance induced by simulated emergent vegetation in open-channel flows. *Journal of Hydraulic Engineering* **137**, 995–1004, https://doi.org/10.1061/(ASCE)HY.1943-7900.0000377 (2010).

37. Nepf, H. M., Ghisalberti, M., White, B. & Murphy, E. Retention time and dispersion associated with submerged aquatic canopies. *Water Resources Research* **43**, https://doi.org/10.1029/2006WR005362 (2007).

38. Nezu, I. & Sanjou, M. Turburence structure and coherent motion in vegetated canopy open-channel flows. *Journal of Hydro-Environment Research* **2**, 62–90, https://doi.org/10.1016/j.jher.2008.05.003 (2008).

39. James, C., Birkhead, A., Jordanova, A. & O'sullivan, J. Flow resistance of emergent vegetation. *Journal of Hydraulic Research* **42**, 390–398, https://doi.org/10.1080/00221686.2004.9728404 (2004).

40. Järvelä, J. Flow resistance of flexible and stiff vegetation: a flume study with natural plants. *Journal of Hydrology* **269**, 44–54, https://doi.org/10.1016/S0022-1694(02)00193-2 (2002).

41. Baptist, M. *et al*. On inducing equations for vegetation resistance. *Journal of Hydraulic Research* **45**, 435–450, https://doi.org/10.1080/00221686.2007.9521778 (2007).

42. Carollo, F., Ferro, V. & Termini, D. Flow resistance law in channels with flexible submerged vegetation. *Journal of Hydraulic Engineering* **131**, 554–564, https://doi.org/10.1061/(ASCE)0733-9429(2005)131:7(554) (2005).

43. Cheng, N.-S. Calculation of drag coefficient for arrays of emergent circular cylinders with pseudofluid model. *Journal of Hydraulic Engineering* **139**, 602–611, https://doi.org/10.1061/(ASCE)HY.1943-7900.0000722 (2012).

44. Katul, G. G., Poggi, D. & Ridolfi, L. A flow resistance model for assessing the impact of vegetation on flood routing mechanics. *Water Resources Research* **47**, https://doi.org/10.1029/2010WR010278 (2011).

45. Klopstra, D., Barneveld, H., Van Noortwijk, J. & Van Velzen, E. Analytical model for hydraulic roughness of submerged vegetation. In *27th IAHR Congress*, 775–780 (HKV Consultants, 1996).

46. Konings, A. G., Katul, G. G. & Thompson, S. E. A phenomenological model for the flow resistance over submerged vegetation. *Water Resources Research* **48**, https://doi.org/10.1029/2011WR011000 (2012).

47. Nepf, H. M. & Ghisalberti, M. Flow and transport in channels with submerged vegetation. *Acta Geophysica* **56**, 753–777, https://doi.org/10.2478/s11600-008-0017-y (2008).

48. Schoneboom, T., Aberle, J. & Dittrich, A. Hydraulic resistance of vegetated flows: Contribution of bed shear stress and vegetative drag to total hydraulic resistance. In *Proceedings of the international conference on fluvial hydraulics river flow* (2010).

49. Van Velzen, E., Jesse, P., Cornelissen, P. & Coops, H. Hydraulic resistance of vegetation in floodplains, part 2: Background document version 1–2003. *Ministry of Transport, Public Works and Water Management, Institute for Inland Water Management and Waste Water Treatment, report* (2003).

50. Chapman, J. A., Wilson, B. N. & Gulliver, J. S. Drag force parameters of rigid and flexible vegetal elements. *Water Resources Research* **51**, 3292–3302, https://doi.org/10.1002/2014WR015436 (2015).

51. Wang, W.-J., Huai, W.-X., Thompson, S. & Katul, G. G. Steady nonuniform shallow flow within emergent vegetation. *Water Resources Research* **51**, 10047–10064, https://doi.org/10.1002/2015WR017658 (2015).

52. Boothroyd, R. J., Hardy, R. J., Warburton, J. & Marjoribanks, T. I. Modeling complex flow structures and drag around a submerged plant of varied posture. *Water Resources Research* **53**, 2877–2901, https://doi.org/10.1002/2016WR020186 (2017).

53. Antonarakis, A. S., Richards, K. S., Brasington, J. & Muller, E. Determining leaf area index and leafy tree roughness using terrestrial laser scanning. *Water Resources Research* **46**, W06510, https://doi.org/10.1029/2009WR008318 (2010).

54. Tinoco, R. O., Goldstein, E. B. & Coco, G. A data-driven approach to develop physically sound predictors: Application to depth-averaged velocities on flows through submerged arrays of rigid cylinders. *Water Resources Research* **51**, 1247–1263, https://doi.org/10.1002/2014WR016380 (2015).

55. Etminan, V., Lowe, R. J. & Ghisalberti, M. A new model for predicting the drag exerted by vegetation canopies. *Water Resources Research* **53**, 3179–3196, https://doi.org/10.1002/2016WR020090 (2017).
56. Kim, S. J. & Stoesser, T. Closure modeling and direct simulation of vegetation drag in flow through emergent vegetation. *Water Resources Research* **47**, https://doi.org/10.1029/2011WR010561 (2011).
57. Poggi, D., Porporato, A., Ridolfi, L., Albertson, J. & Katul, G. The effect of vegetation density on canopy sub-layer turbulence. *Boundary-Layer Meteorology* **111**, 565–587, https://doi.org/10.1023/B:BOUN.0000016576.05621.73 (2004).
58. Huai, W.-X., Wang, W.-J., Hu, Y., Zeng, Y.-H. & Yang, Z.-H. Analytical model of the mean velocity distribution in an open channel with double-layered rigid vegetation. *Advances in Water Resources* **69**, 106–113, https://doi.org/10.1016/j.advwatres.2014.04.001 (2014).
59. Ishikawa, Y., Mizuhara, K. & Ashida, S. Effect of density of trees on drag exerted on trees in river channels. *Journal of Forest Research* **5**, 271–279, https://doi.org/10.1007/BF02767121 (2000).
60. Lee, J., Roig, L., Jenter, H. & Visser, H. Drag coefficients for modeling flow through emergent vegetation in the florida everglades. *Ecological Engineering* **22**, 237–248, https://doi.org/10.1016/j.ecoleng.2004.05.001 (2004).
61. Wu, F., Shen, H. & Chou, Y. Variation of roughness coefficients for unsubmerged and submerged vegetation. *Journal of hydraulic Engineering* **125**, 934–942, https://doi.org/10.1061/(ASCE)0733-9429(1999)125:9(934) (1999).
62. Tanino, Y. & Nepf, H. M. Laboratory investigation of mean drag in a random array of rigid, emergent cylinders. *Journal of Hydraulic Engineering* **134**, 34–41, https://doi.org/10.1061/(ASCE)0733-9429(2008)134:1(34) (2008).
63. Kothyari, U. C., Hayashi, K. & Hashimoto, H. Drag coefficient of unsubmerged rigid vegetation stems in open channel flows. *Journal of Hydraulic Research* **47**, 691–699, https://doi.org/10.3826/jhr.2009.3283 (2009).
64. Zhao, K., Cheng, N., Wang, X. & Tan, S. Measurements of fluctuation in drag acting on rigid cylinder array in open channel flow. *Journal of Hydraulic Engineering* **140**, 48–55, https://doi.org/10.1061/(ASCE)HY.1943-7900.0000811 (2013).
65. Wang, W.-J., Huai, W.-X., Thompson, S., Peng, W.-Q. & Katul, G. G. Drag coefficient estimation using flume experiments in shallow non-uniform water flow within emergent vegetation during rainfall. *Ecological Indicators* **92**, 367–378, https://doi.org/10.1016/j.ecolind.2017.06.041 (2018).
66. Nepf, H. M. & Vivoni, E. R. Flow structure in depth-limited, vegetated flow. *Journal of Geophysical Research: Oceans* **105**, 28547–28557, https://doi.org/10.1029/2000JC900145 (2000).
67. Ferreira, R. M., Ricardo, A. M. & Franca, M. J. Discussion of "laboratory investigation of mean drag in a random array of rigid, emergent cylinders" by yukie tanino and heidi m. nepf. *Journal of Hydraulic Engineering* **135**, 690–693, https://doi.org/10.1061/(ASCE)HY.1943-7900.0000021 (2009).
68. Stoesser, T., Kim, S. & Diplas, P. Turbulent flow through idealized emergent vegetation. *Journal of Hydraulic Engineering* **136**, 1003–1017, https://doi.org/10.1061/(ASCE)HY.1943-7900.0000153 (2010).
69. Dunn, C. *Experimental determination of drag coefficients in open channel with simulated vegetation*. Master's thesis (1996).
70. López, F. & García, M. Mean flow and turbulence structure of open-channel flow through non-emergent vegetation. *Journal of Hydraulic Engineering* **127**, 392–402, https://doi.org/10.1061/(ASCE)0733-9429(2001)127:5(392) (2001).
71. Meijer, D. Flumes studies of submerged vegetation. In *PR121.10*, *HKV*, *Lelystad* (*in Dutch*) (1998).
72. Murphy, E., Ghisalberti, M. & Nepf, H. M. Model and laboratory study of dispersion in flows with submerged vegetation. *Water Resources Research* **43**, https://doi.org/10.1029/2006WR005229 (2007).
73. Shimizu, Y., Tsujimoto, T., Nakagawa, H. & Kitamura, T. Experimental study on flow over rigid vegetation simulated by cylinders with equi-spacing. In *Proceedings of the Japan Society of Civil Engineers*, vol. 438, 31–40 (1991).
74. Stone, B. M. & Shen, H. T. Hydraulic resistance of flow in channels with cylindrical roughness. *Journal of Hydraulic Engineering* **128**, 500–506, https://doi.org/10.1061/(ASCE)0733-9429(2002)128:5(500) (2002).
75. Yan, J. *Experimental study of flow resistance and turbulence characteristics of open channel flow with vegetation*. Thesis (2008).
76. Yang, S.-Q. & Chow, A. T. Turbulence structures in non-uniform flows. *Advances in Water Resources* **31**, 1344–1351, https://doi.org/10.1016/j.advwatres.2008.06.006 (2008).
77. Kubrak, E., Kubrak, J. & Rowiński, P. M. Vertical velocity distributions through and above submerged, flexible vegetation. *Hydrological Sciences Journal* **53**, 905–920 (2008).
78. Okamoto, T. & Nezu, I. Flow resistance law in open-channel flows with rigid and flexible vegetation. In *River Flow 2010*, Dittrich, A., Koll, K. A., Aberle, J. & Geisenhainer, P. (eds), 261–268 (Proceedings of the International Conference on Fluvial Hydraulics, Braunschweig, Germany, 2010).
79. Järvelä, J. Effect of submerged flexible vegetation on flow structure and resistance. *Journal of Hydrology* **307**, 233–241, https://doi.org/10.1016/j.jhydrol.2004.10.013 (2005).
80. Carollo, F., Ferro, V. & Termini, D. Flow velocity measurements in vegetated channels. *Journal of Hydraulic Engineering* **128**, 664–673, https://doi.org/10.1061/(ASCE)0733-9429(2002)128:7(664) (2002).
81. Kouwen, N., Unny, T. & Hill, H. M. Flow retardance in vegetated channels. *Journal of the Irrigation and Drainage Division* **95**, 329–344 (1969).
82. Yang, W. & Choi, S.-U. A two-layer approach for depth-limited open-channel flows with submerged vegetation. *Journal of Hydraulic Research* **48**, 466–475, https://doi.org/10.1080/00221686.2010.491649 (2010).
83. Cheng, N.-S. Representative roughness height of submerged vegetation. *Water Resources Research* **47**, https://doi.org/10.1029/2011WR010590 (2011).
84. Nepf, H. M. Drag, turbulence, and diffusion in flow through emergent vegetation. *Water Resources Research* **35**, 479–489, https://doi.org/10.1029/1998WR900069 (1999).
85. Raupach, M. Drag and drag partition on rough surfaces. *Boundary-Layer Meteorology* **60**, 375–395, https://doi.org/10.1007/BF00155203 (1992).
86. Zdravkovich, M. *Flow around circular cylinders: Applications* 2 (Oxford University Press, Oxford, England, 2000).

Acknowledgements

Author Contributions

Wang contributed to the main work of study design, experiments, data collection, analyses and manuscript writing. Peng, Huai, Katul and Liu provided comments on the study design, experiments, analyses and improved the manuscript. Qu and Dong contributed to the data collection and data analyses.

Additional Information

Supplementary information accompanies this paper at https://doi.org/10.1038/s41598-019-41477-7.

Competing Interests: The authors declare no competing interests.

Publisher's note: Springer Nature remains neutral with regard to jurisdictional claims in published maps and institutional affiliations.